

Flat-detector computed tomography in the assessment of intracranial stents: comparison with multi detector CT and conventional angiography in a new animal model

Tobias Struffert · Sabine Ott · Edyta Adamek ·
Marc Schwarz · Tobias Engelhorn · Stephan Kloska ·
Yu Deuerling-Zheng · Arnd Doerfler

Received: 26 October 2010 / Accepted: 8 January 2011 / Published online: 2 March 2011
© European Society of Radiology 2011

Abstract

Objective Careful follow up is necessary after intracranial stenting because in-stent restenosis (ISR) or residual stenosis (RS) is not rare. A minimally invasive follow-up imaging technique is desirable. The objective was to compare the visualisation of stents in Flat Detector-CT Angiography (FD-CTA) after intravenous contrast medium injection (i.v.) with Multi Detector Computed Tomography Angiography (MD-CTA) and Digital Subtracted Angiography (DSA) in an animal model.

Methods Stents were implanted in the carotid artery of 12 rabbits. In 6 a residual stenosis (RS) was surgically created. Imaging was performed using FD-CTA, MD-CTA and DSA. Measurements of the inner and outer diameter and cross-section area of the stents were performed. Stenosis grade was calculated.

Results In subjective evaluation FD-CTA was superior to MD-CTA. FD-CTA was more accurate compared with DSA than MD-CTA. Cross-sectional area of the stent lumen was significantly larger ($p < 0.05$) in FD-CTA in comparison to MD-CTA. Accurate evaluation of stenosis was impossible in MD-CTA. There was no statistically significant difference in the stenosis grade of DSA and FD-CTA.

Conclusion Our results show that visualisation of stent and stenosis using intravenous FD-CTA compares favourably with DSA and may replace DSA in the follow-up of patients treated with intracranial stents.

Keywords Angiography · Flat detector computed tomography · Animal model · Multislice computed tomography · Intracranial stent

Introduction

Intracranial stents are used for treatment of atherosclerotic disease in increasing numbers [1]. Despite a high technical success rate in-stent restenosis (ISR) may occur in about 30% [2, 3]. Also, residual stenosis (RS) is not rare [1]; therefore, a careful follow-up of is mandatory. The method of choice is conventional digital subtraction angiography (DSA) [4], but this invasive method has the disadvantage of a moderate to high cost. It also carries a low complication rate but the complications can be serious [5]. Therefore, a non-invasive alternative method for is highly desirable.

Magnetic resonance angiography in the assessment of stents is impaired by metal artefacts and therefore not useful [6]. In-vitro studies of stents demonstrated that the minimum diameter for reliable visualisation of the lumen using Multi Detector Computed Tomography Angiography (MD-CTA) was 4.0 mm [4]. The visualisation of the stent lumen is limited due to artificial lumen narrowing (ALN) because of blooming artefacts [7]. Blooming artefacts result in stent struts that appear thicker than they are [8]. New generation Multi Detector CT scanners (MDCT) offered improved visualisation [9]. But the visualisation is limited despite improved MDCT techniques. Therefore DSA remains the gold standard [10].

T. Struffert (✉) · S. Ott · E. Adamek · M. Schwarz ·
T. Engelhorn · S. Kloska · A. Doerfler
Department of Neuroradiology,
University of Erlangen-Nuremberg,
Schwabachanlage 6,
91054 Erlangen, Germany
e-mail: tobias.struffert@uk-erlangen.de

Y. Deuerling-Zheng
Siemens AG, Healthcare Sector,
Siemensstr. 1,
91301 Forchheim, Germany

Recently, Flat-Detector Computed Tomography (FD-CT) has been introduced into clinical routine [11]. Most often they are installed as angiographic systems. Flat detectors have a much smaller detector element size [11]. Therefore these detectors have the physical feature to provide excellent visualisation in high contrast structures with superior spatial resolution. There are many publications concerning the visualisation of stents by FD-CT [12–14]. The idea of obtaining FD-CT with intravenous contrast medium application to achieve an MD-CTA-like image impression is obvious. To the best of our knowledge, a comparison of FD-CT and MDCT after intravenous contrast medium application in the assessment of intracranial stents has not been published. The purpose of the study was to evaluate the visualisation of the stent and stenosis lumen using FD-CTA in comparison to MD-CTA and DSA. We here describe a new surgical technique to create an artificial stenosis in this animal model.

Materials and methods

The study was approved by the local Animal Protection Committee. Twelve New Zealand White Rabbits (4–5 kg body weight) were used. The common carotid artery of these animals has a diameter of 2.5 to 3 mm, within the same range as human intracranial arteries. The feasibility of imaging procedures in these rabbits is well described [15–17].

All animals received aspirin and clopidogrel as an anticoagulation therapy 3 days before stent placement. The animals were anaesthetised by subcutaneous injection of ketamine (80 mg/kg body weight) and xylazine (7 mg/kg body weight). To achieve vascular access the right femoral artery and vein were surgically exposed. A 4F introducer sheath was placed in the artery. A microcatheter (Tracker Excel 14; Boston Scientific/Target, Fremont, CA, USA) was advanced to the left common carotid artery. After selective DSA a 300-cm exchange wire (Synchro Standard; Boston Scientific/Target, Fremont, CA, USA) was placed. We used the Wingspan stent system (Wingspan™; Boston Scientific/Target, Fremont, CA, USA). This device is a self-expandable nitinol stent with markers for increased visibility. Our goal was to implant one stent per animal to avoid any incident that may influence the imaging procedure. We used stents 3 mm in diameter and 15 or 20 mm in length. Furthermore, in six of the 12 animals surgically we created an artificial stenosis that may resemble a residual stenosis. In these six animals a Gateway Balloon Dilatation catheter (Gateway™; Boston Scientific/Target, Fremont, CA, USA) with a diameter of 1.5 mm was placed inside the stent (Fig. 1). The carotid artery was surgically exposed. The balloon was inflated to serve as a spacer and than ligation of the exposed carotid artery was performed. A control

DSA series was obtained. The microcatheter and the introducer sheath were removed and the femoral artery was ligated. To avoid superposition of venous structures during intravenous contrast medium injection using an ear vein [18], we punctured the femoral vein using a standard i.v. cannula (Vasofix Safety®, 20 G, B. Braun Melsungen AG, Melsungen, Germany). This cannula was used for FD-CT and MDCT imaging, then the animals were sacrificed.

Imaging procedure

DSA

We used a biplane flat detector angiography system (Axiom Artis dBA; Siemens Healthcare, Forchheim, Germany). Frame rate was two frames per second. We injected intra-arterial manually using a 1 ml syringe. Due to a dead space of 0.2 ml of the microcatheter and a remaining volume of 0.2 ml within the syringe an amount of 0.5 ml of non-ionic contrast material (Imeron® 300, Bracco Altana Pharma GmbH, Konstanz, Germany) was injected into the artery.

Intravenous FD-CTA

FD-CTA data acquisition was carried out using the 20sDR-H program with the following parameters: 20-second rotation time, projection on 30×40 cm detector size, 217° angular range, increment 0.4°/image. Images were obtained with and without intravenous contrast medium. We used the identical parameters of contrast medium injection (1 ml/kg body weight, followed by 4 ml saline flush, injection rate of 1 ml/s) as described before [19]. Meaning that 4 to 5 ml of non diluted contrast was injected into the venous system. The passage through the heart and lung leads to a prolonged perfusion of the aortic arch covering the entire 20 s acquisition time. We used non-ionic contrast material (Imeron®). As a mean delay time of 4 s from vein to the aortic arch is published [17, 19], we used 4 s of delay time before the FD-CTA run was started. Postprocessing was performed with a dedicated workstation (syngo MMWP, InSpace 3D software; Siemens AG Healthcare Sector, Forchheim, Germany). Postprocessing resulted in an isotropic volume data set with a batch of about 450 slices, slice thickness 0.1 mm, field of view 80 mm and 512×512 matrix. We used the identical reconstruction parameters as described before [19]. After DSA and FD-CTA the animals were transferred to the CT suite.

Multi detector computed tomography angiography

To eliminate the contrast material before MD-CTA the rabbits were hydrated using a 10-ml saline flush. After a

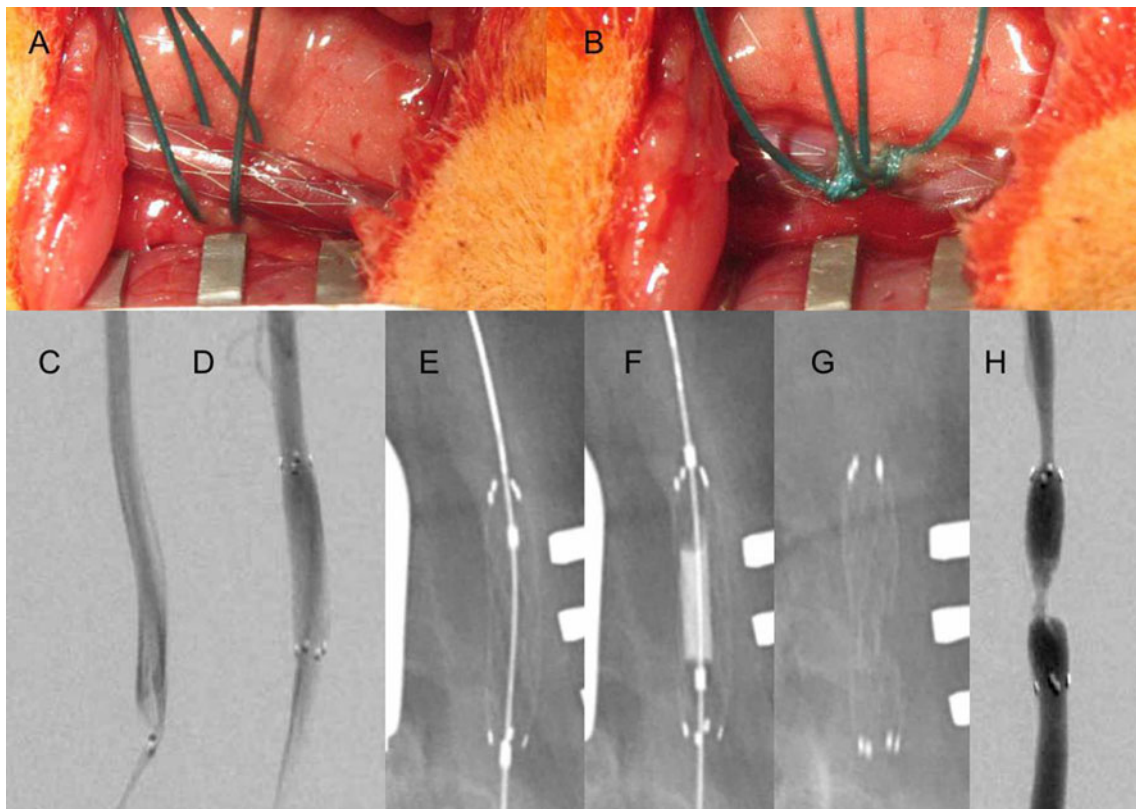


Fig. 1 Creation of an artificial stenosis: in **a** the stent is visible within the common carotid artery. The stent is deployed (**c** before, **d** after stenting) and then a balloon (**e**) is placed and inflated (**f**). Then ligation

(**b**) is performed. Note the compressed stent struts (**g**). The result of this surgical procedure is resembling a residual stent stenosis (**h**)

delay of 45 min the animals were examined by MD-CTA. We performed imaging with and without contrast medium application. CT was performed by a Siemens Somatom Sensation 64 (64 rows, Siemens Healthcare, Forchheim, Germany). We used an application as proposed by the manufacturer and others [4, 7, 9, 10] with the following parameters: 160 mAs, 100 kV, rotation time 0.5 s, 64×0.6 mm collimation, pitch 1.3, reconstruction increment 0.4 mm, slice thickness 0.75 mm, total exposure time of 4 s, matrix 512×512, field of view 80 mm, kernel B40 resulting in a batch of about 450 slices. Bolus tracking was used at the level of the heart. We used the identical contrast medium parameters as for FD-CT [19].

Postprocessing

Both FD-CTA and MD-CTA images were postprocessed using a dedicated workstation (syngo MMWP, Siemens AG Healthcare Sector, Forchheim, Germany). Multiplanar reformations (MPR) with 1-mm slice thickness were reconstructed in the axial and sagittal plane [4, 7, 8, 10, 19]. We tried to find matching slice positions, which is not perfectly possible because of transportation e.g. different positioning of the animals. We reconstructed the data sets

with and without contrast medium application. Technical details were deleted from the images so that it was not possible to recognise the technique used. The DSA images before and after stent placement were stored. Two experienced neuroradiologists (referred to as RAD1 and RAD2) independently evaluated the images on the workstation. The reviewers had the opportunity to adjust windowing in FD-CTA and MD-CTA individually for each data set.

Data evaluation

The reviewers had to perform a subjective evaluation of the images. Additional measurements of the stents were performed. The images before and after stenting had to be evaluated subjectively for the following details:

Any signs of vascular damage (e.g. dissections, thrombus formation) had to be recorded. Deployment status of the stent had to be evaluated. The visualisation of the stent lumen on FD-CTA and MD-CTA images was evaluated with a subjective dichotomised scale for quality. The reviewers had to evaluate if the visualisation of the stent lumen after contrast medium injection was (1) highly opacified, (2) contrast visible and suitable for diagnostic evaluation, or (3) no contrast between the native and

contrast-enhanced images visible and therefore not of diagnostic value. The visibility of the lumen of the stenosis had to be evaluated to be (1) clearly visible, (2) impaired by blooming but still sufficiently visible or (3) impaired by blooming and not evaluable. To assess blooming artefacts the reviewers were asked to evaluate the visualisation on axial reconstructions to assess stent struts to be (1) clearly visible, (2) not clearly delineated or (3) have a ring-like appearance. Should any beam hardening artefacts be visible, the reviewers were asked to describe the location and the appearance to be (1) visible but not impairing lumen visibility, (2) clearly visible and impairing lumen visibility or (3) massive artefacts with obvious impaired image quality preventing diagnostic assessment of the lumen.

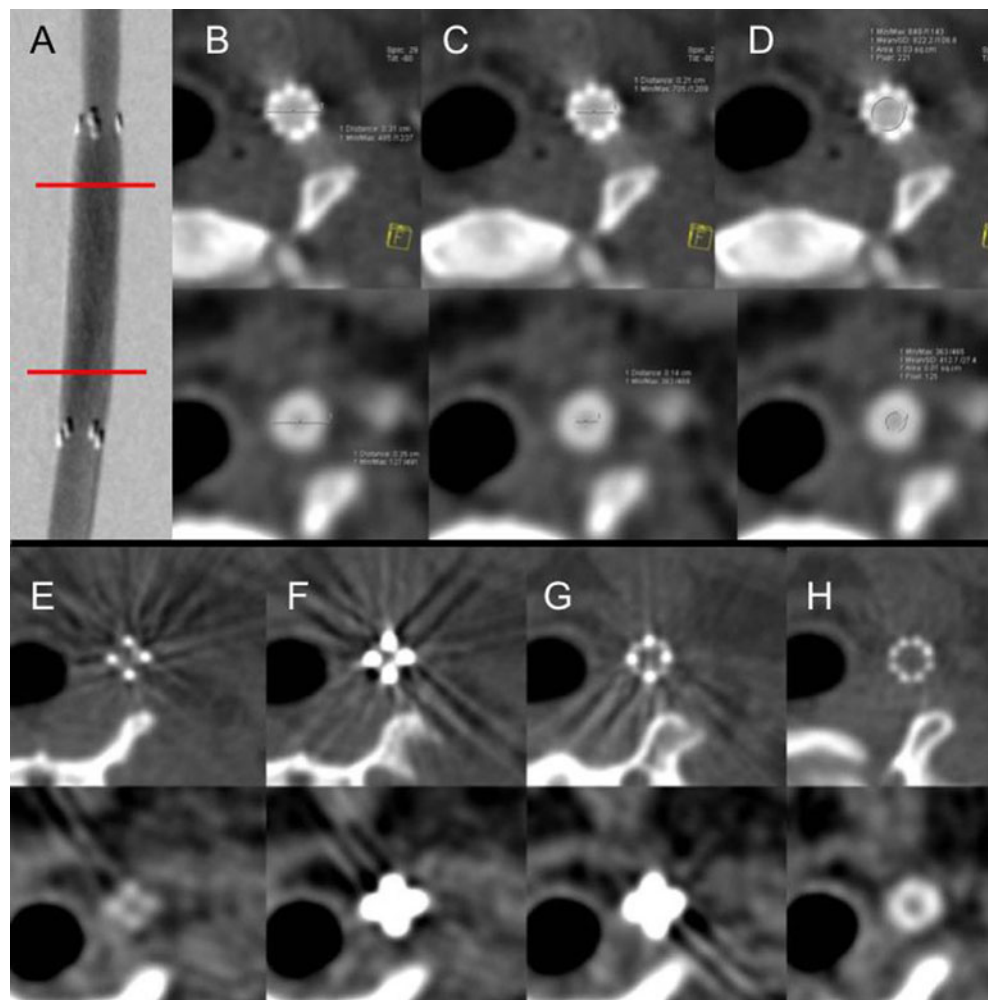
The Wingspan™ stent system has very thin struts that are hardly recognisable on DSA images [8] (Fig. 2a). The reviewers were asked to measure the diameter of the proximal and distal stent on DSA images. In FD-CTA and MD-CTA the stent device itself is visible (Fig. 2). Blooming effects result in stent struts that appear thicker

than they are [8] meaning that an inner and outer part of the stent can be recognised. The reviewers were asked to measure the inner and outside diameter of the stent close to the proximal and the distal orifice on FD-CTA and MD-CTA images. The reviewers were asked to measure the area of the proximal and distal lumen. Measurements were performed using standard tools of the workstation. The reviewers were asked to measure the grade of stenosis using the following equation: $\text{percentage stenosis} = (1 - D_{\text{stenosis}}/D_{\text{normal}}) \times 100$. D_{stenosis} is the diameter at its most severe site. D_{normal} is the diameter of the proximal stent [20].

Statistics

Values were expressed as mean \pm standard deviation (SD). Statistical analysis was carried out by SPSS 14.0 using calculation of Pearson's correlation coefficient (r) for inter- and intra-observer correlation. The Wilcoxon test was used to compare the measurements of the stents by the different methods.

Fig. 2 Measurements were performed close to the proximal and distal orifices of the stent (a, red lines). Inner and outer diameter and cross-section area (b–d) were measured. In e–h axial images with 1-mm slice thickness at the markers of a stent demonstrate beam hardening artefacts with typical streak-like appearance. In the upper row FD-CTA is displayed showing that this type of artefact is less severe than in MD-CTA (lower row)



Results

Stent deployment was successfully performed in all 12 animals. Creation of a stenosis was performed in six of the 12 animals (Fig. 1). Imaging data could be obtained in all animals for all imaging techniques.

Signs of vascular damage were not recognised in any animal. The subjective evaluation of the DSA images revealed in both reviewers that all stents were deployed completely and adopted to the vessel wall (Fig. 1d). The stenosis in 6 animals was perfectly visible (Fig. 1h). Vascular injuries were not visible, but in two of the six animals with stenosis creation we recognised vasospasms of the distal carotid artery due to surgical manipulation (Fig. 1h).

The subjective evaluation of the FD-CTA and MD-CTA also demonstrated complete deployment of the stents (Figs. 3 and 4). Both reviewers described the FD-CTA images as highly opacified, but the MD-CTA images as opacified and suitable for diagnostic evaluation. On all FD-CTA images the stent struts were visible (Figs. 3 and 4a and b) while on MD-CTA images the struts were not clearly visible and the stent appeared like a hyperdense ring due to blooming artefact (Figs. 3. and 4c and d). Especially on axial reconstructions beam hardening artefacts of the stent markers were visible (Fig. 2e–h). On FD-CTA artefacts were clearly visible and impairing lumen visibility. On MD-CTA the artefacts were

massive and evaluation of the lumen at the proximal and distal orifice of the stent was impossible.

In all the animals with stenosis the lumen at the stenosis was clearly visible on FD-CTA (Fig. 4). On MD-CTA the lumen of the stenosis was impaired by blooming and not visible. Therefore measurements on MD-CTA were not meaningful. A measurement of the stenosis grade was made by comparing the inner diameter proximally and at the stenosis on FD-CTA and DSA.

The results of the diameter measurements showed a high inter-observer correlation (Fig. 5a). We found high correlation coefficients (r) in comparison of the measurements of REV I and II (Table 1). The standard deviations of all data points overlapped (Fig. 5a). The combined measurements of both reviewers expressed as mean with standard deviation are given in Fig. 5b. The value of the external diameter of the stents in FD-CTA was lower while the measurements of the internal diameter of FD-CTA were significantly higher in comparison to MD-CTA ($p < 0.05$). The diameter measurements of DSA compared significantly better with the external diameter measurements of FD-CTA ($p < 0.05$). Concerning the area we detected a significant difference ($p < 0.05$) with a larger proximal and distal area in FD-CTA compared with MD-CTA (Fig. 6a).

Concerning the stenosis we did not detect a significant difference in the measurements of REV I and II, but stenosis grade appeared to be slightly higher with FD-CTA which was

Fig. 3 The FD-CTA (a native, b with contrast medium) images show perfect visualisation of the stent lumen and stent struts. On MD-CTA (c native, d with contrast medium) the beam hardening artefacts of the markers and the blooming of the stent struts impair visualisation of the lumen. Corresponding DSA image is shown in Fig. 1d

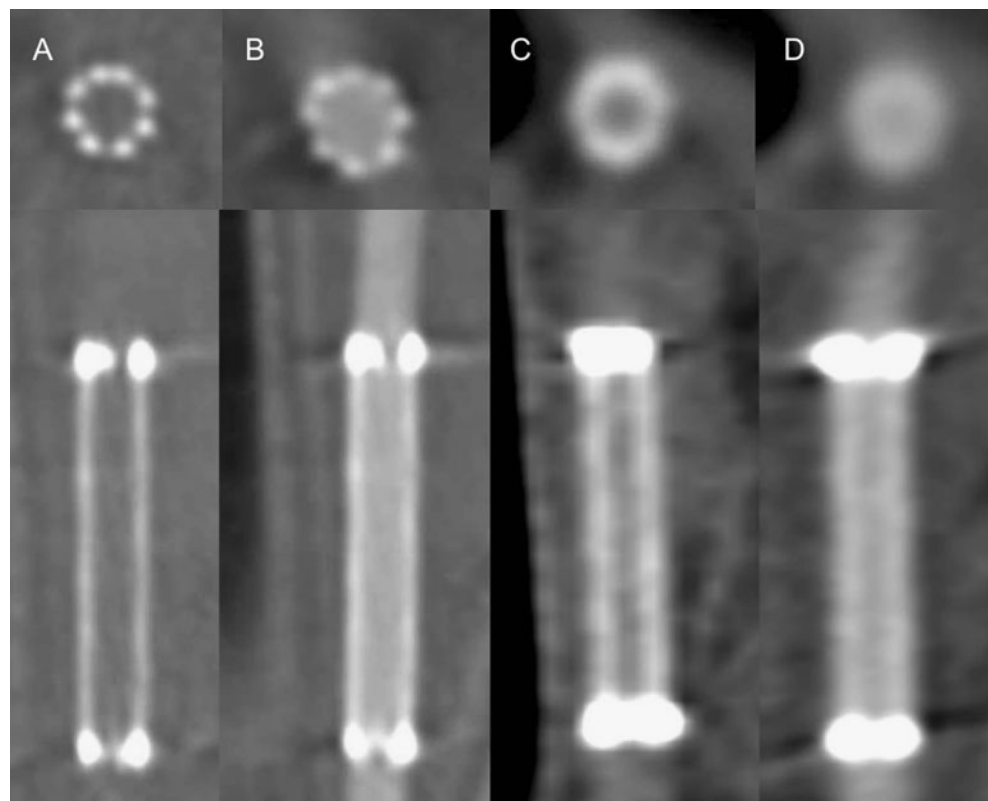


Fig. 4 In **a** (native) and **b** (with contrast medium) a stenosis is displayed on FD-CTA. The residual lumen is visible. On MD-CTA (**c** native, **d** with contrast medium) the lumen of the stenosis is not visible due to blooming artefact. Corresponding DSA image is shown in Fig. 1h

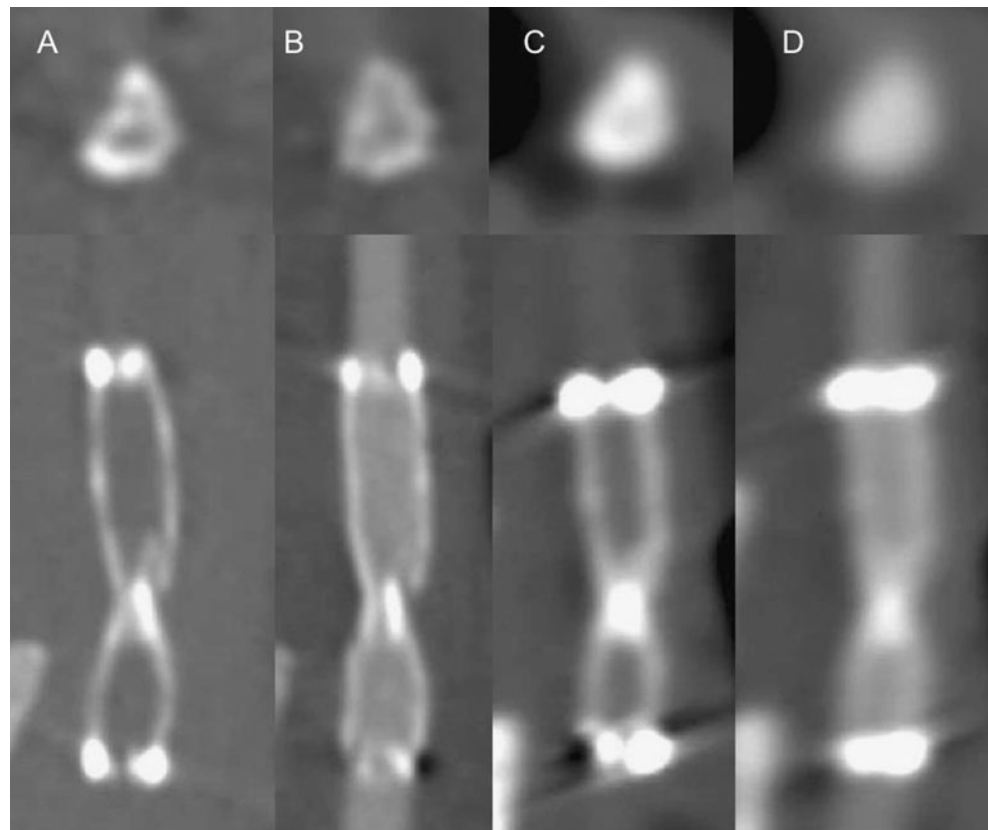


Fig. 5 In **a** the inter-observer agreement is displayed. Mean values of reviewers I and II were not statistically different and showed high correlation values (Table 1). The combined results (**b**) of the measurements of the inner and outer diameter show that MD-CTA values are higher for the outer and lower for the inner diameter in comparison to FD-CTA. DSA compares well with FD-CTA

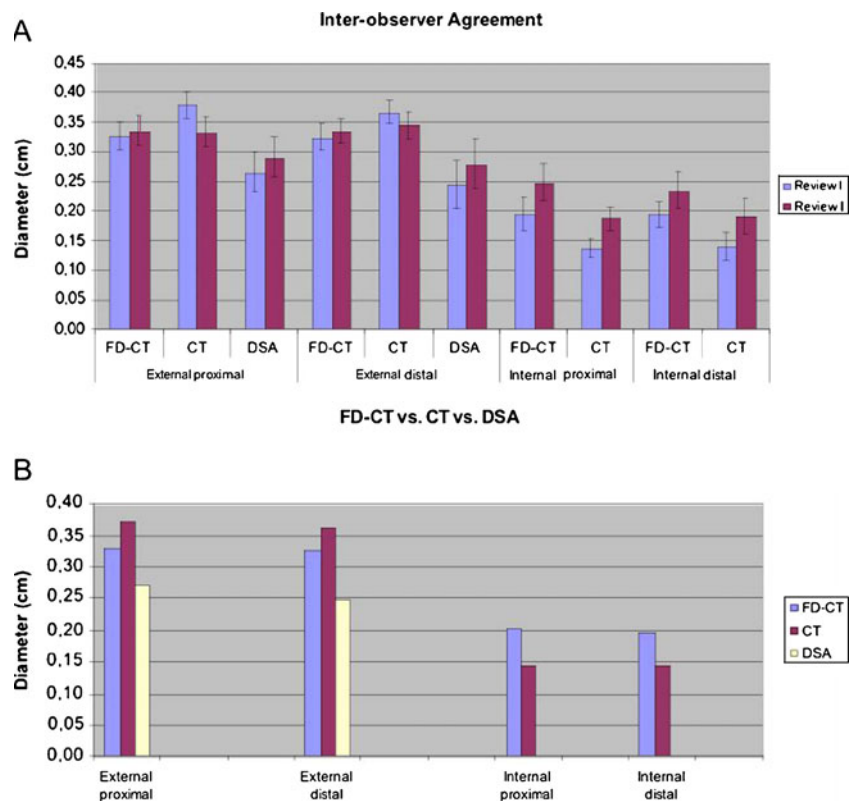


Table 1 Displaying the correlation coefficients (r) of the diameter measurements of REV I and II

Correlation	External proximal	External distal	Internal proximal	Internal distal
FD-CT	0.93	0.95	0.97	0.89
CT	0.8	0.86	0.77	0.83
DSA	0.86	0.96		

not statistically significant. The results (Fig. 6b) expressed as mean with standard deviations are overlapping.

Discussion

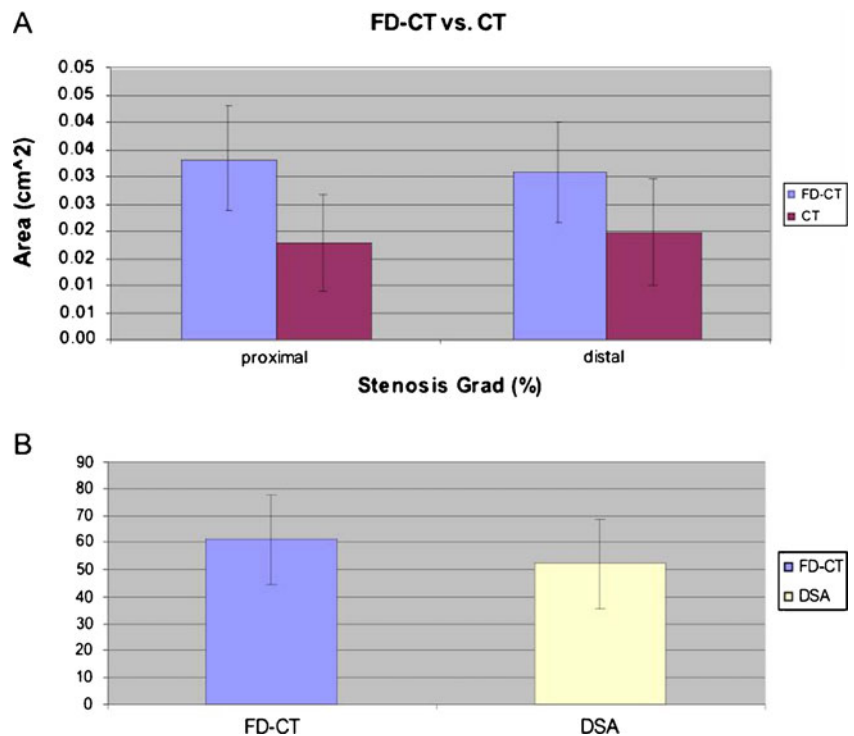
Since FD-CT was introduced into clinical routine, it has become widely used to visualise haemorrhage or endovascular implants [12–14, 21, 22]. It was demonstrated that stents for intracranial use can be depicted in perfect resolution. The idea of using intravenous contrast material to enhance vascular structures by FD-CT is obvious but has rarely been reported [19]. Another publication describes a similar FD-CT application to perform imaging of the brain parenchyma, the intracranial arteries and cerebral perfusion [23]. To our knowledge Buhk et al. [24] were the first to describe the use of intravenous contrast material in FD-CT for imaging of intracranial stents. Struffert et al. described an optimised FD-CT program and published a small series of patients [25]. In these publications a comparison to MDCT is not given and therefore a further

evaluation of FD-CTA in the visualisation of intracranial stents is mandatory.

The feasibility of FD-CTA by using contrast material in a dose comparable to that used in humans has been described in a rabbit model [19]. Additional, imaging procedures in rabbits have been well described [17] and, this model has been used to test new stent devices [26, 27]. Therefore this animal model seems to be appropriate for further evaluation of stents. To date there is only one publication describing a model for creating a carotid artery stenosis [28]. This swine model is not useful for intracranial stents because the vessel diameter of the carotid artery is not appropriate. As a further development of the rabbit model we here describe a new surgical method of creating an artificial stenosis and can show the feasibility of this new model. The procedure is not very demanding and easy to perform.

Our interest was if the dimensions of the stents, the lumen and stenosis would be depicted more accurately on FD-CTA than on MD-CTA compared with the gold standard of DSA. In the subjective evaluation of the native

Fig. 6 The cross sectional area was significantly larger on FD-CTA in comparison to MD-CTA (a). Comparison of stenosis grade between DSA and FD-CTA was not significantly different with a tendency of FD-CTA towards slightly higher values (b)



and contrast-enhanced images it becomes obvious that the opacification in FD-CTA appeared superior to MD-CTA. The contrast enhancement can be perceived more easily on FD-CTA. The stent struts could be recognised on FD-CTA, but not on MD-CTA images. Because of blooming the stents appeared to be ring-like. In the visualisation of the artificial stenotic stents, the lumen could be recognised on FD-CTA while in MD-CTA the lumen could not be seen. Blooming seems to affect MD-CTA images more severe than FD-CTA. Additionally, beam hardening artefacts of the stent markers were more obvious on MD-CTA.

In our series measurements of diameters showed a high correlation between the two reviewers (Table 1). The diameters appear different on FD-CTA and MD-CTA. We found that the inner diameter was smaller and the outer diameter was larger on MD-CTA in comparison to FD-CTA. Measurements of FD-CTA were more accurate compared with DSA than MD-CTA. Additionally, the cross-section area was larger on FD-CTA in comparison to MD-CTA indicating that artificial lumen narrowing is of high impact on MD-CTA [4, 7]. Our results indicate that the dimensions of the stents on FD-CTA comply better with the gold standard of DSA.

There are some shortcomings to our study. The sample size of 12 rabbits is small, but sufficient to demonstrate the superior visualisation of stents using FD-CTA. Signal ratios are interesting to compare the achieved contrast, but measurement of Hounsfield units is not yet possible in FD-CT. The animals were positioned in the z axis (e.g. the carotid artery) of the FD-CT and MDCT systems. We cannot comment on the visualisation of the beam hardening artefacts of the stent markers if placed at a different angle to the z axis.

Our results indicate that FD-CTA compares well with DSA. Obviously MD-CTA is still limited in the visualisation of small stents. It is obvious that imaging of other implants like coils or clips might also be performed with this new imaging technique. We detected beam hardening artefacts of the stent markers impairing image quality on both MD-CTA and FD-CTA. It is well known that beam hardening artefacts are more severe with increasing amounts of implanted metal material [14]. If these beam hardening artefacts could be reduced, visualisation of coils and clips should be possible. Efforts are ongoing to resolve these artefacts [29].

Conclusion

In this new animal model we demonstrated the feasibility of stenosis creation. Our results show that FD-CTA compares well with DSA. MD-CTA is impaired by blooming artefacts and therefore not useful in the visualisation of stents. FD-

CTA with intravenous contrast medium application as a minimally invasive imaging technique may replace DSA in the follow-up of patients treated with these devices.

Acknowledgement The work described in this study was supported by a grant from the ELAN-Fonds, Erlangen, Germany (www.elan.uni-erlangen.de), Project number 07.07.18.1. Boston Scientific/Target supported our work by supporting stents and other angiographic equipment.

References

1. Bose A, Hartmann M, Henkes H, Liu HM, Teng MM, Szikora I et al (2007) A novel, self-expanding, nitinol stent in medically refractory intracranial atherosclerotic stenoses: the Wingspan study. *Stroke* 38:1531–1537
2. Levy EI, Turk AS, Albuquerque FC, Niemann DB, Aagaard-Kienitz B, Pride L et al (2007) Wingspan in-stent restenosis and thrombosis: incidence, clinical presentation, and management. *Neurosurgery* 61:644–650
3. Fiorella DJ, Levy EI, Turk AS, Albuquerque FC, Pride GL Jr, Woo HH et al (2009) Target lesion revascularization after wingspan: assessment of safety and durability. *Stroke* 40:106–110
4. Trossbach M, Hartmann M, Braun C, Sartor K, Hähnel S (2004) Small vessel stents for intracranial angioplasty: in vitro evaluation of in-stent stenoses using CT angiography. *Neuroradiology* 46:459–463
5. Willinsky RA, Taylor SM, TerBrugge K, Farb RI, Tomlinson G, Montanera W (2003) Neurologic complications of cerebral angiography: prospective analysis of 2, 899 procedures and review of the literature. *Radiology* 227:522–528
6. Prabhakaran S, Warrior L, Wells KR, Jhaveri MD, Chen M, Lopes DK (2009) The utility of quantitative magnetic resonance angiography in the assessment of intracranial in-stent stenosis. *Stroke* 40:991–993
7. Hähnel S, Trossbach M, Braun C, Heiland S, Knauth M, Sartor K et al (2003) Small-vessel stents for intracranial angioplasty: in vitro comparison of different stent designs and sizes by using CT angiography. *AJNR Am J Neuroradiol* 24:1512–1516
8. Turk AS, Rowley HA, Niemann DB, Fiorella D, Aagaard-Kienitz B, Pulfer K et al (2007) CT angiographic appearance of in-stent restenosis of intracranial arteries treated with the Wingspan stent. *AJNR Am J Neuroradiol* 28:1752–1754
9. Maintz D, Seifarth H, Flohr T, Krämer S, Wichter T, Heindel W et al (2003) Improved coronary artery stent visualisation and in-stent stenosis detection using 16-slice computed-tomography and dedicated image reconstruction technique. *Invest Radiol* 38:790–795
10. Choo KS, Lee TH, Choi CH, Park KP, Kim CW, Kim S (2009) Assessment of the intracranial stents patency and re-stenosis by 16-slice ct angiography with optimized sharp kernel: preliminary study. *J Korean Neurosurg Soc* 45:284–288
11. Kalender WA, Kyriakou Y (2007) Flat-detector computed tomography (FD-CT). *Eur Radiol* 17:2767–2779
12. Benndorf G, Strother CM, Claus B, Naeini R, Morsi H, Klucznik R, Mawad ME (2005) Angiographic CT in cerebrovascular stenting. *AJNR Am J Neuroradiol* 26:1813–1818
13. Benndorf G, Klucznik RP, Strother CM (2006) Images in cardiovascular medicine: angiographic computed tomography for imaging of underdeployed intracranial stent. *Circulation* 114:e499–e500
14. Richter G, Engelhorn T, Struffert T, Doelken M, Ganslandt O, Hornegger J et al (2007) Flat panel detector angiographic CT for

- stent-assisted coil embolization of broad-based cerebral aneurysms. *AJNR Am J Neuroradiol* 28:1902–1908
15. Cloft HJ, Altes TA, Marx WF, Raible RJ, Hudson SB, Helm GA et al (1999) Endovascular creation of an in vivo bifurcation aneurysm model in rabbits. *Radiology* 213:223–228
 16. Kallmes DF, Helm GA, Hudson SB, Altes TA, Do HM, Mandell JW et al (1999) Histologic evaluation of platinum coil embolization in an aneurysm model in rabbits. *Radiology* 213:217–222
 17. Doerfler A, Becker W, Wanke I, Goericke S, Oezkan N, Forsting M (2004) Multimodal imaging in the elastase-induced aneurysm model in rabbits: a comparative study using serial DSA, MRA and CTA. *Röfo* 176:590–596
 18. Struffert T, Roth C, Romeike B, Grunwald IQ, Reith W (2008) Onyx in an experimental aneurysm model: histological and angiographic results. *J Neurosurg* 109:77–82
 19. Struffert T, Doelken M, Adamek E, Schwarz M, Engelhorn T, Kloska S (2010) Flat-detector computed tomography with intravenous contrast material application in experimental aneurysms: comparison with multislice CT and conventional angiography. *Acta Radiol* 51:431–437
 20. Nguyen-Huynh MN, Wintermark M, English J, Lam J, Vittinghoff E, Smith WS et al (2008) How accurate is CT angiography in evaluating intracranial atherosclerotic disease? *Stroke* 39:1184–1188
 21. Struffert T, Eyupoglu IY, Huttner HB, Engelhorn T, Doelken M, Saake M et al (2010) Clinical evaluation of flat-panel detector compared with multislice computed tomography in 65 patients with acute intracranial hemorrhage: initial results. *J Neurosurg* 113:901–907
 22. Struffert T, Richter G, Engelhorn T, Doelken M, Goelitz P, Kalender WA et al (2009) Visualisation of intracerebral haemorrhage with flat-detector CT compared to multislice CT: results in 44 cases. *Eur Radiol* 19:619–625
 23. Struffert T, Deuerling-Zheng Y, Kloska S, Engelhorn T, Strother CM, Kalender WA et al (2010) Flat detector CT in the evaluation of brain parenchyma, intracranial vasculature, and cerebral blood volume: a pilot study in patients with acute symptoms of cerebral ischemia. *AJNR Am J Neuroradiol* 31:1462–1469
 24. Buhk JH, Lingor P, Knauth M (2008) Angiographic CT with intravenous administration of contrast medium is a noninvasive option for follow-up after intracranial stenting. *Neuroradiology* 50:349–354
 25. Struffert T, Kloska S, Engelhorn T, Deuerling-Zheng Y, Ott S, Doelken M et al (2011) Optimized intravenous flat detector CT for non-invasive visualisation of intracranial stents: first results. *Eur Radiol* 21:411–418
 26. Kühn AL, Roth C, Romeike B, Grunwald IQ (2009) Treatment of elastase-induced intracranial aneurysms in New Zealand white rabbits by use of a novel neurovascular embolization stent device. *Neuroradiology*. doi:10.1007/s00234-009-0605-9
 27. Ahlhelm F, Roth C, Kaufmann R, Schulte-Altendorneburg G, Romeike BF, Reith W (2007) Treatment of wide-necked intracranial aneurysms with a novel self-expanding two-zonal endovascular stent device. *Neuroradiology* 49:1023–1028
 28. Ishii A, Viñuela F, Murayama Y, Yuki I, Nien YL, Yeh DT et al (2006) Swine model of carotid artery atherosclerosis: experimental induction by surgical partial ligation and dietary hypercholesterolemia. *AJNR Am J Neuroradiol* 27:1893–1899
 29. Prell D, Kyriakou Y, Struffert T, Dörfler A, Kalender WA (2010) Metal artifact reduction for clipping and coiling in interventional C-arm CT. *AJNR Am J Neuroradiol* 31:634–639